International Journal of Radiology and Diagnostic Imaging

E-ISSN: 2664-4444
P-ISSN: 2664-4436
www.radiologypaper.com
IJRDI 2024; 7(2): 62-71
Received: 23-06-2024
Accepted: 30-07-2024

Asmaa Oraby
Faculty of Medicine, University of Tanta, Tanta, AL Gharbia, Radiodiagnosis and Medical Imaging Department, Faculty of Medicine, University of Tanta, Tanta, AL Gharbia, Egypt

Noha Abdel Maboud
Department, Faculty of Medicine, Faculty of Medicine, University of Tanta, Tanta, AL Gharbia, Radiodiagnosis and Medical Imaging University of Tanta, Tanta, AL Gharbia, Egypt

Reda Al-Arabawy
Department, Faculty of Medicine, Faculty of Medicine, University of Tanta, Tanta, AL Gharbia, Radiodiagnosis and Medical Imaging University of Tanta, Tanta, AL Gharbia, Egypt

Rasha Dawoud
Department, Faculty of Medicine, Faculty of Medicine, University of Tanta, Tanta, AL Gharbia, Radiodiagnosis and Medical Imaging University of Tanta, Tanta, AL Gharbia, Egypt

Soha Romeih
Department, Faculty of Medicine,Faculty of Medicine, University of Tanta, Tanta, AL Gharbia, Radiodiagnosis and Medical Imaging University of Tanta, Tanta, AL Gharbia, Egypt

Corresponding Author:
Asmaa Oraby
Department Radiodiagnosis and Medical Imaging, Faculty of Medicine, University of Tanta, Tanta, AL Gharbia, Faculty of Medicine, University of Tanta, Tanta, AL Gharbia, Egypt

Assessment of global radial strain by feature tracking cardiac magnetic resonance in patients with myocardial infarction

Asmaa Oraby, Noha Abdel Maboud, Reda Al -Arabawy, Rasha Dawoud and Soha Romeih

DOI: https://doi.org/10.33545/26644436.2024.v7.i3a.399

Abstract
This study aimed to assess global radial strain (GRS) using feature tracking cardiac magnetic resonance (CMR-FT) in patients with myocardial infarction (MI). Between January 2018 and September 2021, 26 MI patients and 20 healthy controls underwent CMR examinations at Tanta University Hospitals. The mean age of the study population was 54 ± 12 years. The study found that the peak GRS in MI patients was significantly lower (25.66 ± 9.54) compared to controls (35.94 ± 5.27, $p< 0.001$). A GRS cut-off of ≤ 34.69 distinguished cases from controls with 83% sensitivity and 75% specificity. Additionally, GRS was significantly correlated with the transmurality of the scar (r= -0.668, $p< 0.001$) and scar percentage (r= -0.750, $p< 0.001$). These findings suggest that CMR-FT-derived GRS analysis is a valuable tool for evaluating myocardial deformation and its relationship with traditional CMR parameters and scar quantification in post-MI patients.

Keywords: Global radial strain, cardiac magnetic resonance, myocardial infarction, feature tracking

Introduction
31% of all global deaths occur due to cardiovascular diseases. Coronary heart disease (CAD), which is marked by the gradual development of atherosclerotic plaques in the coronary arteries, frequently progresses to acute and chronic coronary syndrome (CCS) [1, 2].
A fibrous scar occupying >50% of the segment is considered non-viable for treatment; <50% is considered viable. Assessing myocardial viability is crucial for effective treatment decisions in patients with chronic ischemic left ventricular dysfunction. The LGE sequence, with its high spatial resolution, is the noninvasive gold standard for distinguishing between subendocardial and transmural lesions. A fibrous scar > 50% of the segment is non-viable while ≤ 50% is considered viable [3, 4].
Previous studies in patients with chronic ischemic dysfunction found no improvement in the transmural LGE scar post-revascularization treatment, rendering it unresponsive to procedures like PCI and CABG [3, 5-7].
The assessment of RWMA on film images and LGE scar percentage relies heavily on visual evaluation, necessitating contrast administration and additional analysis time [8].
To visualize scar tissue, gadolinium-based contrast agents must be administered intravenously as there is no alternative for this in cardiac MRI at present. LGE sequences are time-consuming and typically use more than 50% of the examination time due to the required delay of 10-15 minutes after the administration of contrast agents, which is important for contrast retention in the scar In addition, the intravenous use of gadolinium-based contrast agents is limited in patients with acute and chronic renal failure [9, 10].
Certain applications of intravenous contrast agents may result in a potentially lethal allergic reaction. Attention is growing towards alternative sign-detection methods based on commonly used Chinese images [11-13].
Myocardial stress behavior is regionally altered due to reduced contractility caused by the formation of scar tissue from myofibroblasts that replace myocytes after an infarct [14, 15].
During systole, the circumferential and longitudinal strains in a healthy myocardium have negative values, while the radial strain shows positive values for thickening.

Scar tissue results in a regional alteration of myocardial stress behavior due to reduced myocardial contractility. Myofibroblasts, which replace myocytes after an infarct [14, 15].

Patients and methods

Between January 2018 and September 2021, a total of 26 patients and 20 controls got CT scans at Tanta University Hospitals' Diagnostic Radiology & Medical Imaging Department. Twenty more healthy participants were included in the trial. Obtained informed consent and permission from the ethics committee.

Inclusion criteria

- Any patient who underwent CMR assessment of myocardial viability based on scarring.

Exclusion criteria

- There are patients who are known to be contraindicated for magnetic resonance imaging (MRI). These include patients who have an implanted ferromagnetic device, cardiac pacemakers that are incompatible with MRIs, cochlear implant patients, and patients with non-MRI compatible pacemakers.
- Individuals with a GFR of less than 30 ml/min/1.73 m2 who have renal failure.
- Patients with severe uncontrollable cardiac arrhythmia.
- Patients with severe claustrophobia.
- Patient with associated pathology that may added factor for strain impairment such as associated aortic stenosis

Methods

All the following data were obtained from saved files on database

- Personal history: age and sex.
- Risk factors.
- Systemic hypertension (HTN).
- Diabetes mellitus.
- Dyslipidemia.
- Smoking.
- Body mass index (BMI).
- CMR examinations.

CMR examination

Toshiba "Vantage Titan" MRI scanner 1.5T was used to exam the studied patients at (CMR) at the department of Diagnostic Radiology & Medical Imaging at Tanta university hospitals

Scenario of CMR examination

Patient preparation before CMR

- All subjects were requested to fast for 4 hours before the CMR examination.
- Renal function tests are done to exclude renal impairment; contrast should not be given to patients with a glomerular filtration rate less than 30 ml/min/1.73 m2.
- A written safety list to exclude any MRI contraindications is read, filled out and signed by the patient.
- The examination was explained in full detail to the patient by the attending physician.
- Explanation of the possible side effects of the contrast agent include headache, paranesthesia, dizziness, itching, nausea, vomiting, warmth, coldness, or pain at the injection site.
- Insertion of an ante-cubital intravenous cannula is done, the dose of contrast given was 0.15 mmol/Kg.
- Patients were instructed to leave all metallic objects outside the scanner.

During the procedure

1. Patient's position and preparation

- All patients were examined in the supine position, headfirst without any movement to ensure that the planned examination region matched the actual scanned region.
- Four ECG leads are connected. Satisfactory ECG tracing should be obtained for optimal image resolution by shaving and cleaning the skin as necessary, spacing the caps apart enough to minimize potential interference voltage differences between them when in the magnet, and correctly placing the flaps to get it right. The defined QRS complex is of relatively high amplitude.
- The pear-shaped sensor was used when the apnea sequences were applied. It was placed in the maximum area of respiratory movement under the spiral. A strap was used to secure the sensor. The respiratory signal was verified when the respiratory wave was displayed on the monitor and used to detect the patient's breathing rate and synchronize the instructions to hold the breath with the patient's capabilities. The patient's breath-hold exercises are performed under the nurse's supervision.
- Hearing protection is provided.
- A cardiac coil is applied

2. Image Acquisition

a) Localizers (static images)

Axial, coronal, sagittal, and oblique plane localising imaging using ECG-gated steady-state free precession (SSFP), these images were important for planning the other sequences, used for anatomy survey, extracardiac findings as well as to confirming adequacy of the imaging coil size, including:

- Localizer 15 slices.
- Localizer 60 slices.
- **Localizer false 2 chamber:** 1 slice from axial localizer, parallel to ventricular septum.
- **Localizer false short axis:** (Multi-slice covering the ventricles from localizer false 2 chamber and axial localizer, perpendicular to the longitudinal axis of the left ventricle).

b) Cine images

- **Cine pictures (Dynamic images):** Breath-hold, retrospective ECG-triggered cine SSFP using the subsequent configurations: The following planes have the following parameters: 6 mm-thick sections with 9 mm gaps, a 360 mm field of view, a 256 208-matrix size, a 40 msec repetition time, 1.3 msec echo duration, and a 60° flip angle.
- **4-chamber:** (1 slice passes through the mitral valve and apex on two chamber localizers in the left ventricle, obliquely bisecting left ventricular anterolateral wall and right ventricular apex on short axis localizer).
- **2-chamber:** (1 slice parallel to ventricular septum on short axis localizer, bisecting the left ventricle is

visualized via the mitral valve and the apex in a four-chamber cine).

- **3-chamber:** (1 slice bisecting the LVOT and postero-lateral LV wall on short axis localizer, LVOT as well as the coronal localizer images and LV apex at false 2-ch localizer).

c) LGE

6 to 10 minutes post-injection of 0.15 mmol/kg gadolinium contrast agent, delayed enhancement images were acquired utilizing a gradient-prepared rapid echo sequence with inversion recovery.

5 minutes post-contrast, the optimal inversion time for delayed enhancement imaging was determined using a multiple inversion (Cine IR) recovery sequence (TI scout). Images of 2, 3, and 4 cameras and SAX LGE, with a contrast recovery-phase recovery inversion sequence, were acquired to cover the entire ventricle.

Interpretation

- Initially, the visual evaluation was carried out by viewing locators and cine images as movies in a single view, zooming, panning and changing the contrast for individual images and also the cine series, then carry out a quantitative evaluation after the treatment.

1. Visual assessment of myocardial segmental abnormalities was performed using long- and short-axis cine images based on hypokinesia, akinesia, or dyskinesia.
2. **Ventricular volumes and function**

- Ventricular volumes and function were measured using Circle CVI 42 software after processing.
- The parameters derived from the calculation were LV end-diastolic volume, LV end-systolic volume, LV stroke volume, LV ejection fraction, LV end-diastolic volume index, LV end-systolic volume index, and LV stroke volume index.

3. Evaluated short-axis stack images ± axial stack images with computer-aided analysis software.
4. **Feature tracking LV strain analysis:** A global longitudinal, circumferential and radial analysis with monitoring characteristics of 16 myocardial AHA segments in each case's analysis was conducted using Segment software (Medviso, Lund, Sweden).

Radial strain

An analysis of the radial deformation by monitoring the characteristics of the myocardium 16 segmented into basal, middle, and apical levels at the end of the diastolic phase was analyzed with the quantification of the maximum global radial deformation and the results were calculated automatically. Monitoring the functionality of the Segment software. The systolic thickness of the left ventricular myocardium determines the radial strain's positive value.

LGE

Signs of LGE were assessed visually to estimate the percentage of lesions in each myocardial segment using short-axis imaging. A myocardium with a scar percentage below 50% was considered viable, while a myocardium with a scar percentage above 50% was deemed nonviable [4]. Quantification of LGE lesions by scar percentage by Segment software (Medviso, Lund, Sweden).

Results

The mean age of the study population, ranging from 27 to 89 years, is presented in Table 1&2 as 54 ± 12, 16 of them were male (62%) and 10 were female (38%). Approximately 73% were hypertensive, 58% were diabetic 4% had hyperlipidemia, 73% were smokers and 4% were alcoholic.

Table 1: Study population characteristics

	Patients (n = 26)		Control (n = 20)	
	No.	**%**	**No.**	**%**
Sex				
Male	16	62	13	65.0
Female	10	38	7	35.0
Age(years)				
Min.-Max.	27.0-89.0		19.0-72.0	
Mean ± SD.	54 ± 12		33 ± 14.03	
Median (IQR)	54.5 (46.0-62)		25.0 (23.0-42.0)	

IQR: Inter quartile range
SD: Standard deviation

Table 2: Distribution of the studied cases according to risk factors in patients group (n = 26)

Risk factors	No.	%
Diabetic	15	58
HTN	19	73
Smoking	19	73
Dyslipdemia	1	4
Acholic	1	4

Amony the whole cases, 14 (54%) were anterior STEMI and 12 (46%) were inferior STEMI.

Table 3: Territorial classification of the studied patients (n = 26)

Clinical	No.	%
Anterior STEMI	14	54.0
Inferior STEMI	12	46.0

The peak GRS of the patient group was significantly lower (25.66 ± 9.54) compared to the controls (35.94 ± 5.27), $P<$ 0.001. The table (4) depicts the findings.

Table 4: Comparison between patients and controls according to strain parameters.

	Patients (n = 26)	Control (n = 20)	Test of Sig.	P
GRS				
Min.-Max.	3.83-51.13	22.89-42.02	t= 6.785*	<0.001*
Mean ± SD.	25.66 ± 9.54	35.94 ± 5.27		
Median (IQR)	24.61 (17.99-33.32)	36.95 (33.45-39.67)		

The ROC curve differentiated cases from controls (Figure 1). A radial strain cut-off point of ≤ 34.69, with sensitivity 83% and specificity 75%, yields an AUC of 0.821 (95% CI: 0.739-0.903). (Table 4).

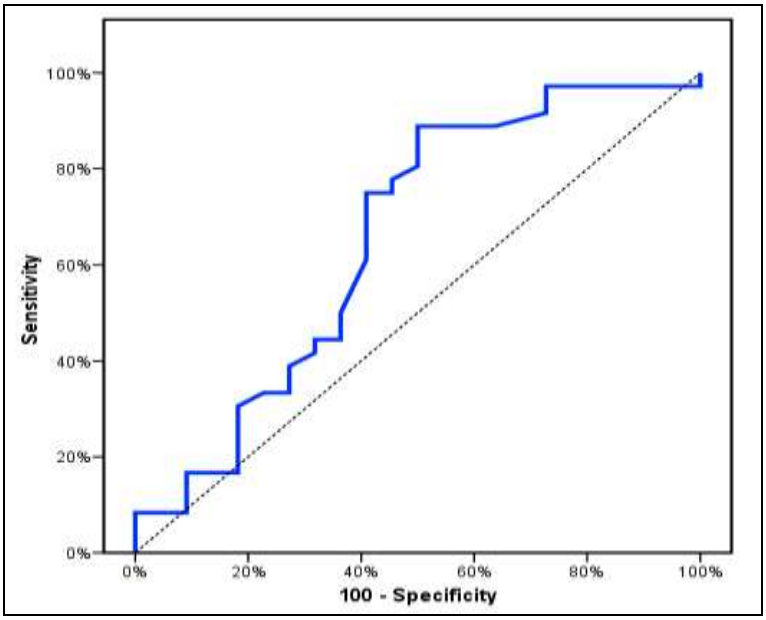

Fig 1: Show the sensitivity and Specificity

Table 5: Prognostic performance for GRS to discriminate cases from control.

	AUC	P	95% C.I	Cut off	Sensitivity	Specificity
GRS	0.821	<0.001*	0.739-0.903	≤34.69	83.0	75.0

There was significant correlation between GRS and transmurality of scar and scar percentage (r= -0.668, p= < 0.001 and r= -750, p= < 0.001 respectively). Table (5).

Table 5: Correlation GRS and different parameters in patients group (n= 26)

	GRS	
	R	P
Transmurality of scar	-0.668	<0.001*
Scar percentage (%)	-0.750	<0.001*

r: Pearson coefficient r_s: Spearman coefficient*: Statistically significant at $p \leq 0.05$

Subgrouping patients group into two groups; patients with GRS ≤34.69 (n= 14) and GRS >34.69 (n= 12) was done.
On comparing the two groups, there was statistical significance as regard sex, traditional CMR parameters including (EF, SVI, ESVI and EDVI), p = <0.019, p= < 0.001, P = 0.005, P = 0.001 and <0.001 respectively and as well as scar percentage, p = <0.001, these findings were illustrated at Table (6).

Table 6: Comparison between the two studied groups (GRS ≤34.69 and GRS > 34.69)

	GRs				Test of Sig.	P
	≤34.69 (n =14)		>34.69 (n = 12)			
	No.	%	No.	%		
EF						
Min.-Max.	20.0-71.0		48.0-69.0		t=8.796*	<0.001*
Mean ± SD.	41.06 ± 12.63		59.65 ± 6.58			
Median	42.0		61.0			
SVI						
Min.-Max.	25.0-59.0		35.0-59.0		t=2.878*	0.005*
Mean ± SD.	39.61 ± 7.23		45.12 ± 6.96			
Median	39.0		44.0			
ESVI						
Min.-Max.	15.0-211.0		20.0-65.0		U=239.50*	<0.001*
Mean ± SD.	64.58 ± 34.96		32.94 ± 11.59			
Median	56.0		32.0			
EDVI						
Min.-Max.	51.0-264.0		58.0-124.0		U=312.0*	<0.001*
Mean ± SD.	104.1 ± 35.11		76.35 ± 16.61			
Median	98.0		70.0			
Scar quantification						
Min.-Max.	2.30-44.0		1.30-23.40		U=246.50*	<0.001*
Mean ± SD.	22.78 ± 10.81		10.44 ± 6.28			
Median	23.0		9.0			

SD: Standard deviation t: Student t-test U: Mann Whitney test
χ^2:Chi square test FE: Fisher Exact

The ROC curves for significant variables determined with GRS (GRS ≤ 34.69) distinguished patients with higher EF values (EF ≤ 56), resulting in an AUC of 0.906 (95% CI = 0.847-0.965), p=<0.001, with a sensitivity of 87.85% and specificity of 70.59%. The sensitivity and specificity of a cutoff value of SVI ≤42 are 66.27% and 64.71%, respectively, with an AUC of 0.704, 95% CI =0.580-0.829, and p<0.008. A cutoff value of 37 or higher for ESVI (with an AUC of 0.830, 95% CI of 0.742-0.918, p<0.001) was found to have a sensitivity of 79.52% and specificity of 70.59%. A cutoff value of 81 for EDVI was established with an AUC of 0.779, a 95% confidence interval of 0.673-0.884, and a significance level of <0.001.

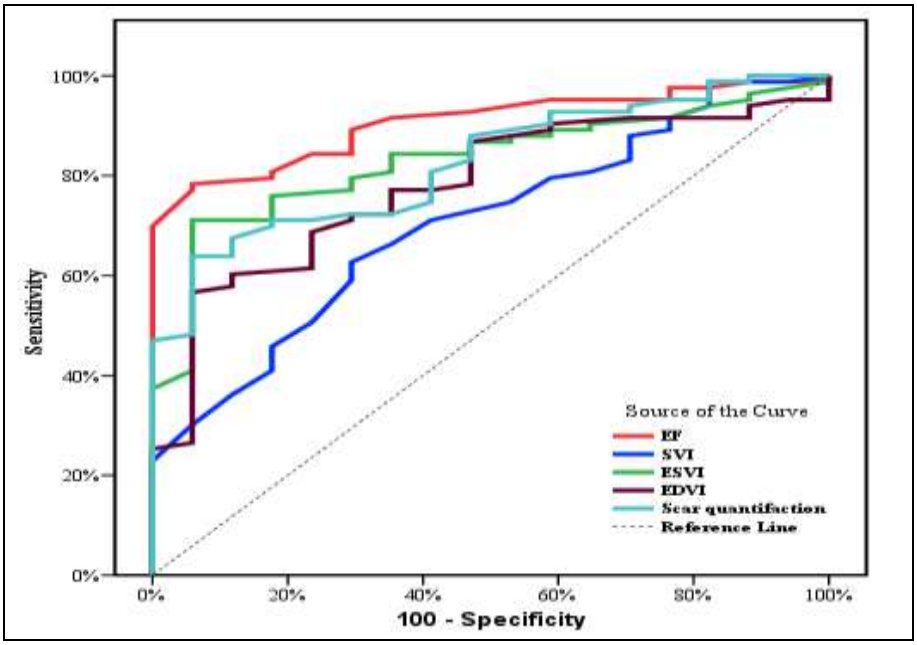

Fig 5: ROC curve for different parameters to predict GRs (≤34.69)

Sensitivity 77.11%, specificity 64.71%. A cutoff value scar percentage >14.2% was determined with AUC= 0.825, 95% CI =0.736- 0.915), p=<0.001 with sensitivity 72.29%, specificity 70.59%. These findings were listed in Table (7).

Table 7: Prognostic performance for different parameters to predict GRs (≤34.69) in the whole sample (n= 26).

	AUC	P	95% C.I	Cut off	Sensitivity	Specificity
EF	0.906	<0.001*	0.847 -0.965	≤56	87.95	70.59
SVI	0.704	0.008*	0.580-0.829	≤42	66.27	64.71
ESVI	0.830	<0.001*	0.742-0.918	>37	79.52	70.59
EDVI	0.779	<0.001*	0.673-0.884	>80	77.11	64.71
Scar quantification	0.825	<0.001*	0.736-0.915	>14.2	72.29	70.59

Case 1

21-year-old female patient, with LV EF of 65% (control).

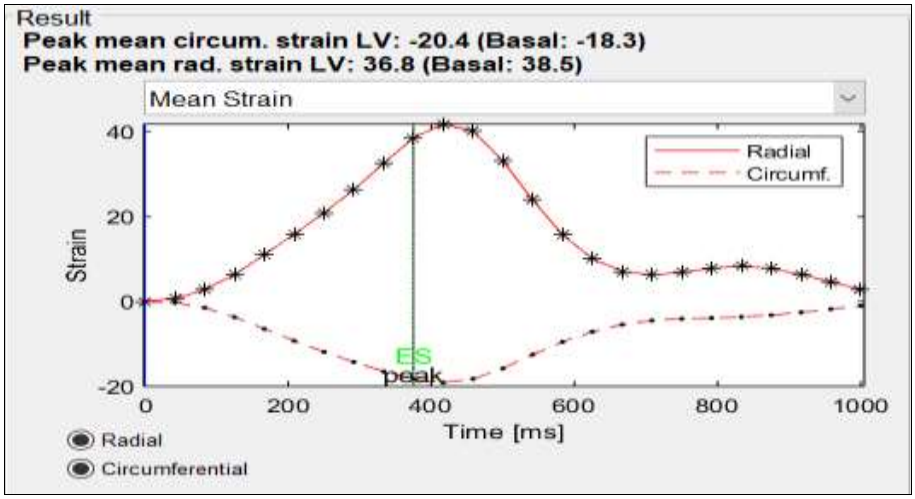

Fig 3: Graphical plotting of the global circumferential and radial strain against time. Peak global radial strain was within the normal values (-20.4 and 36.8 respectively)

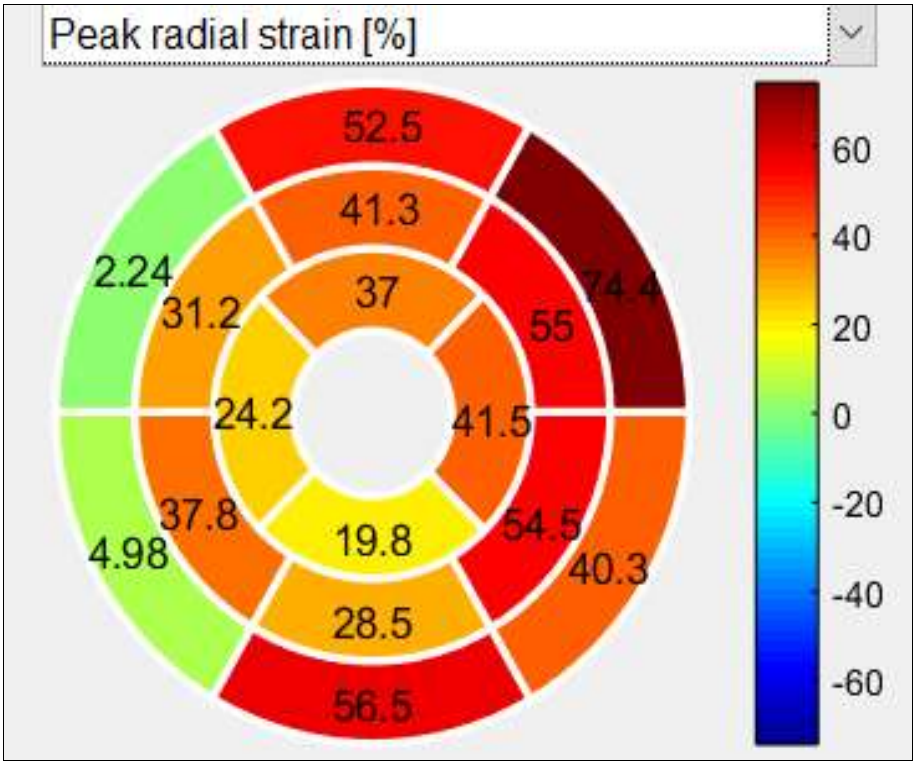

Fig 4: Bull's eye display of the segmental radial strain; all segments are coded with variable degrees of red and orange except basal segments which could be explained by the tethering effect of the mitral annulus fibrous structures.

Case No. 2

A 69-year-old Female patient with previous anterior STEMI 3 months before the current CMR. Volumetric assessment by CMR; EF= 29%, ESVI=103, EDVI= 146 and SVI= 42.

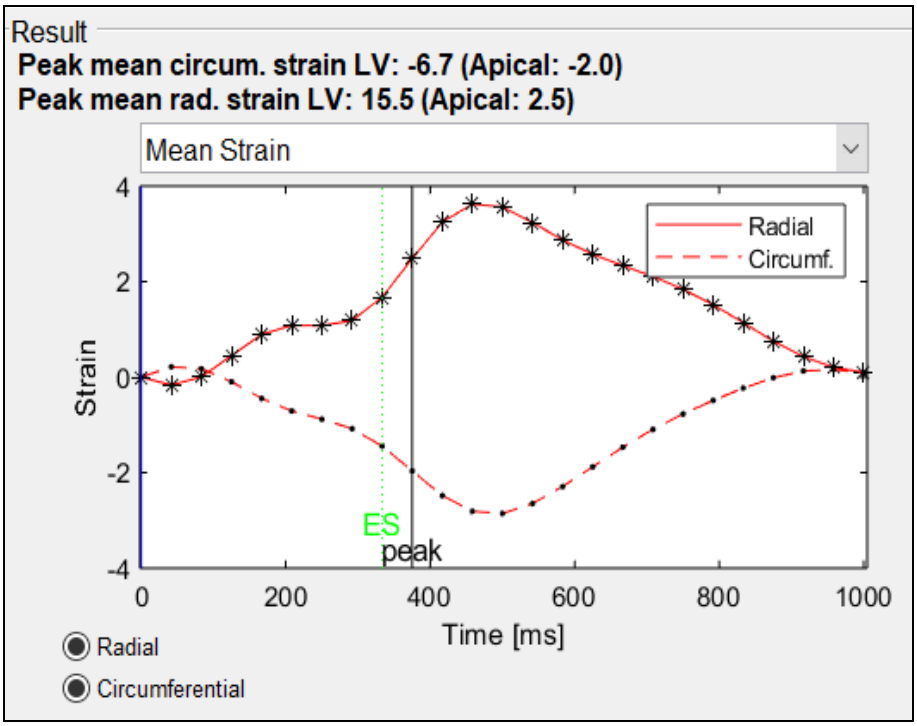

Fig 4: Graphical plotting of the global circumferential and radial strain against time. Peak global circumferential and radial strains are of -6.7 and 15.5 respectively.

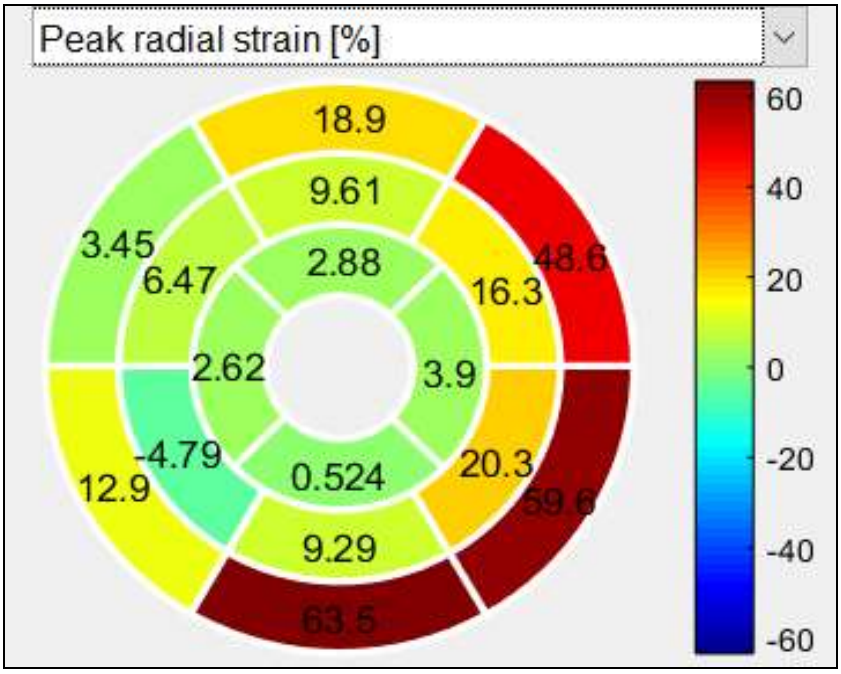

Fig 5: Bull's eye display of the segmental radial strain; all segments are coded with variable variable shades of red, orange, yellow and green.

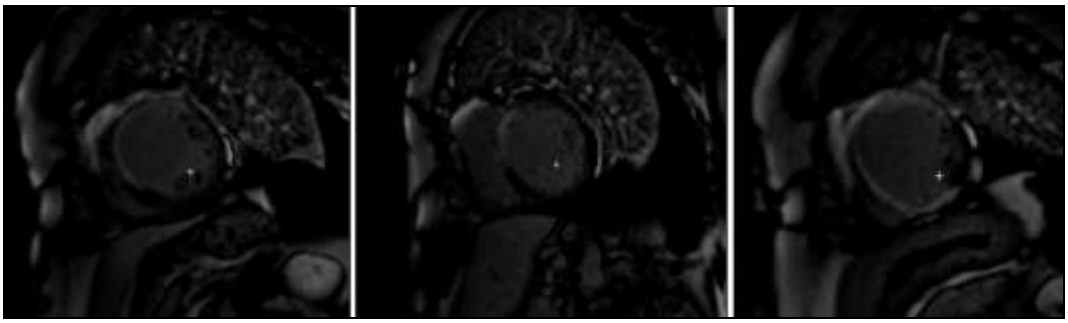

Fig 6: Basal, mid and apical views of LGE showing basal antero-septal, mid anterior and antero-septal as well as apical anterior, septal and inferior with focal lateral transmural enhancement consistent with non-viable LAD territory.

Case No. 3

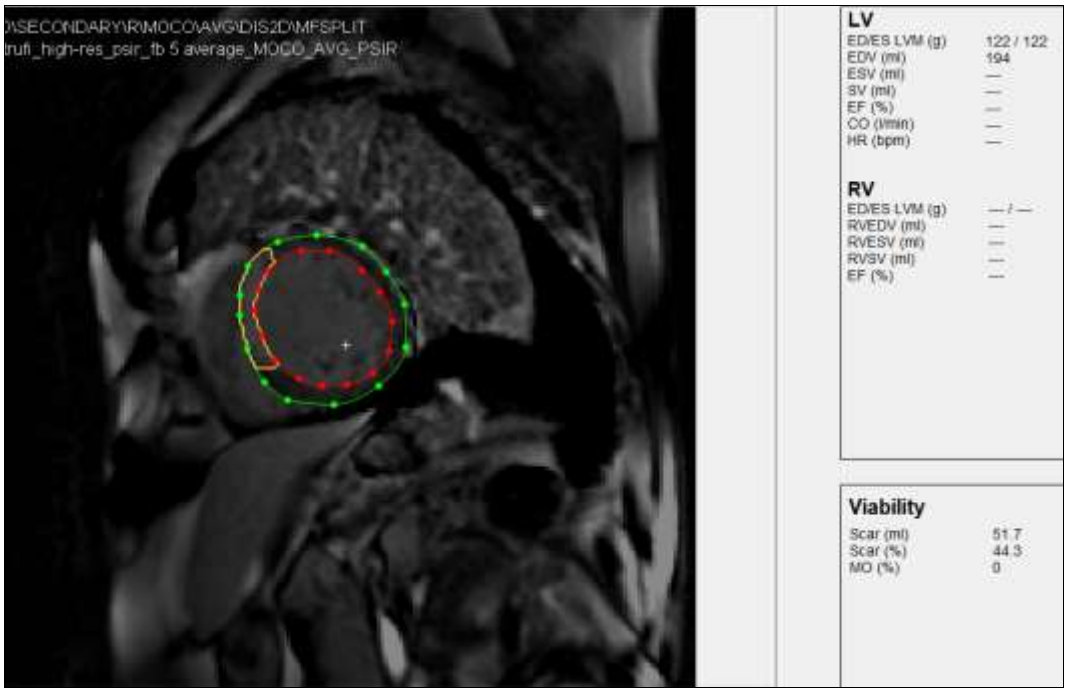

Fig 7: Quantitative assessment of myocardial scar = 44.3% of total myocardial mass

Case No. 3

49-year-old female patient, with a history of previous inferior STEMI underwent primary PCI 2 months before CMR examination. Volumetric assessment by CMR; EF= 45%, ESVI=47, EDVI= 85 and SVI= 39.

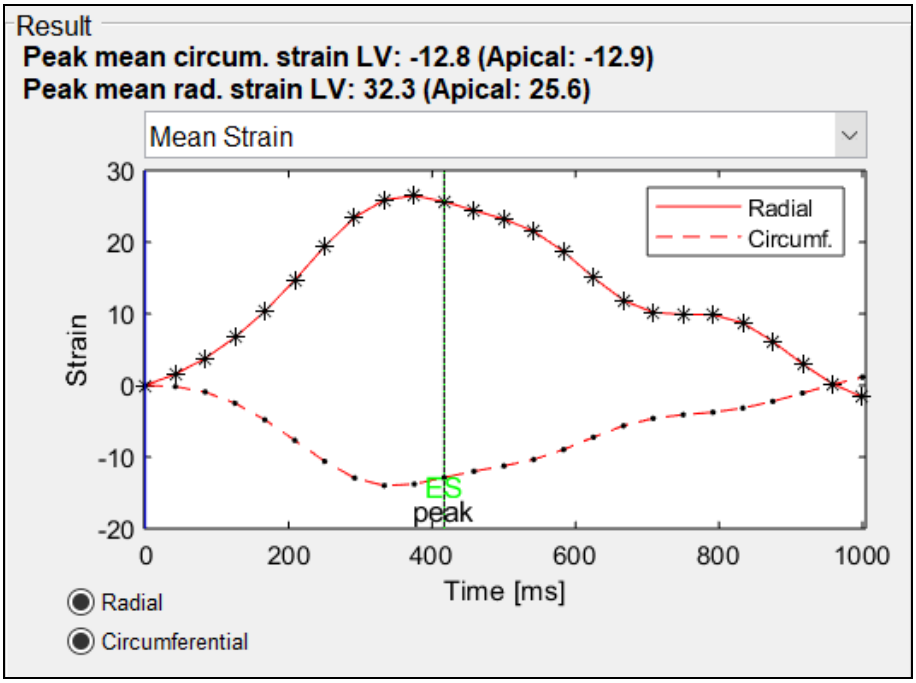

Fig 8: Graphical plotting of the global radial strain against time. Peak global circumferential and radial strains is of 32.3.

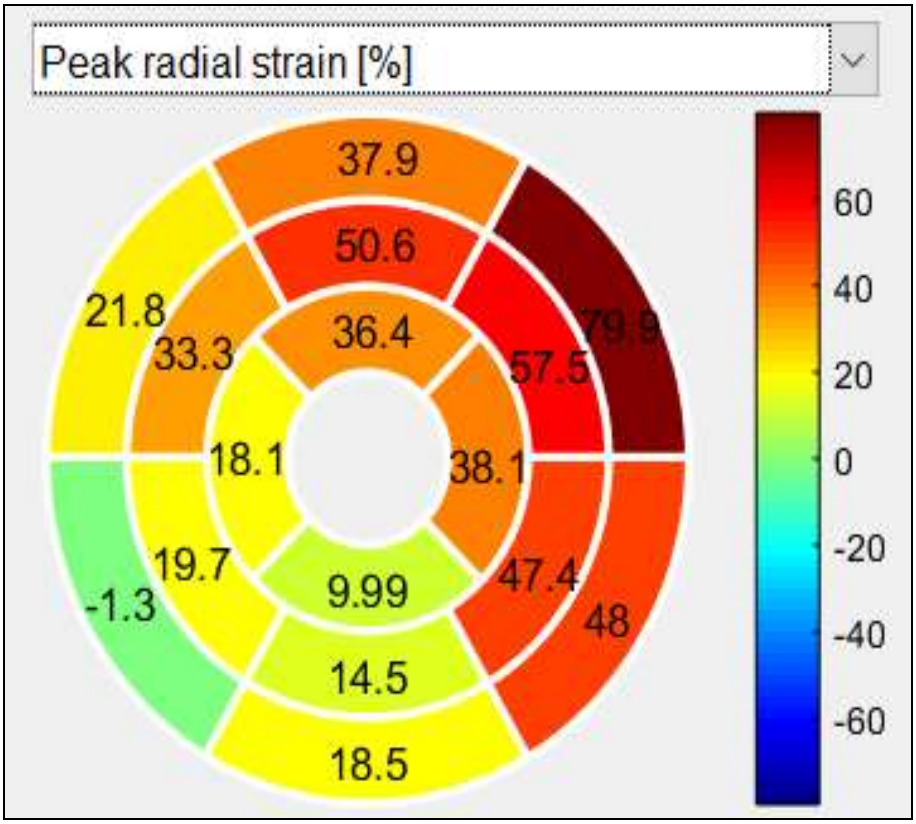

Fig 9: Bull's eye display of the segmental radial strain; all segments are coded with variable shades of red, orange, yellow and green.

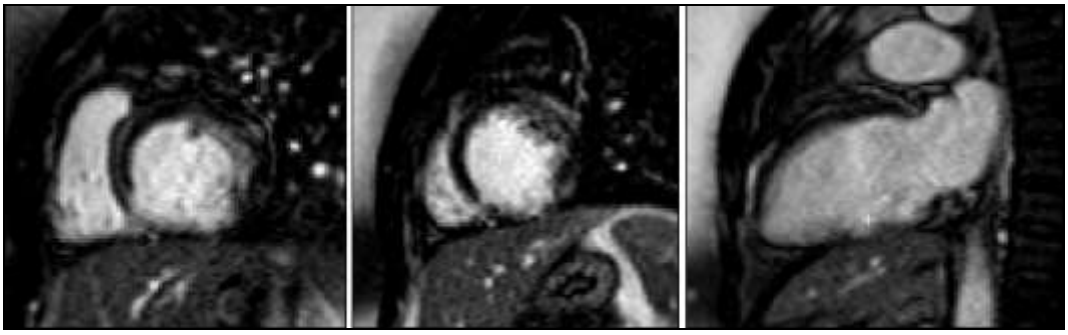

Fig 9: Basal, Mid and 2-chamber views of LGE showing Transmural enhancement of the basal, mid and apical ventricular segments of the inferior wall with focal transmural enhancement of basal and mid-infero-septal segments alongside subendocardial scar > 50% of the apex consistent with non-viable RCA territory

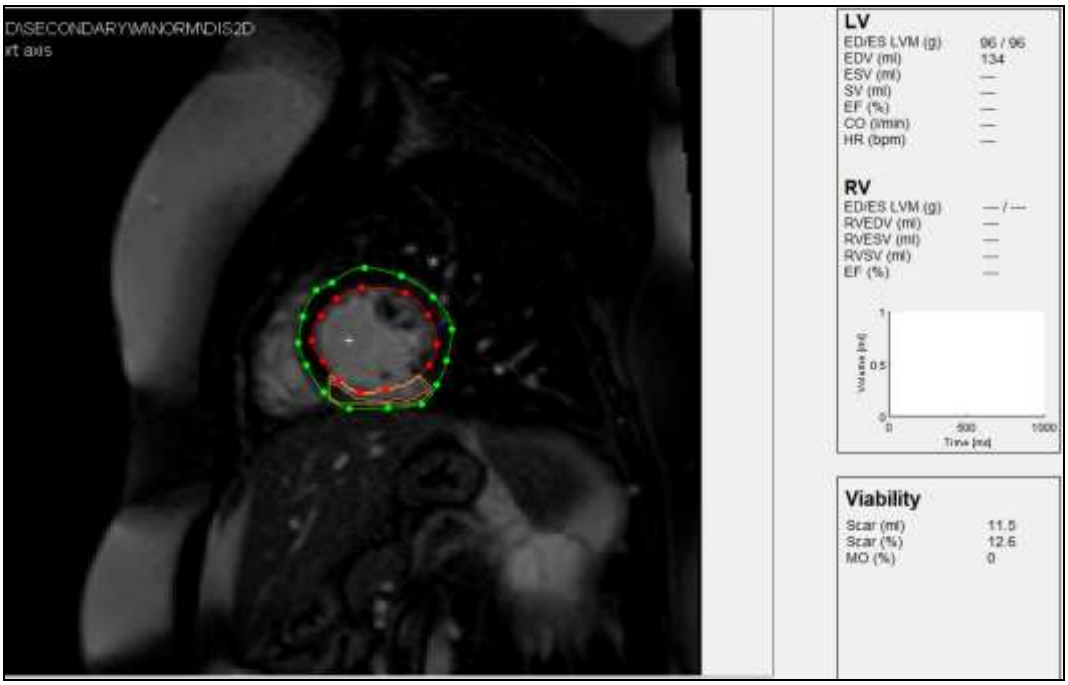

Fig 10: Quantitative assessment of myocardial scar = 12.6% of total myocardial mass

Discussion

Three dimensions of myocardial deformation are measured by strain: Radial strain measures thickening from endocardium to epicardium, longitudinal strain measures shortening from base to apex, and circumferential strain assesses systolic shortening along the ventricle's short axis. Age, sex, and LV loading circumstances often affect all strain variations [16, 17].

In contrast to LVEF, strain is a more thorough assessment that looks at three distinct orientations of myocardial deformation that match the geometry of the heart's fibres. In this sense, strain may be a useful addition to LVEF in the evaluation of myocardial infarction patients [18].

The main findings of our study could be summarized as follow:

(I): Our study adopted a cutoff point of normal LV strain, by comparing our patients group to an age and sex matched control group, below which there would be abnormal myocardial deformation (34.69 for GRS).

(II): GRS was negatively correlated with myocardial fibrosis as well as percentage of the scar (p= < 0.001).

For myocardial strain to be clinically useful, normal ranges of strain and in healthy populations are needed.

Normal cut-off values of radial strain ranging between 25 to 30% are considered within normal, which was lower than our determined GRS cutoff which was 34.69 [19].

A recent publication by Tantawy SW *et al.* [20] used feature tracking CMR to test GRS in patients with chronic ischemia, they found a significant difference between patient and control groups (23.11 ± 6.59% vs. 31.72 ± 5.52%), p=0.001. This was somewhere close to peak GRS attained at our patient and control group (25.66 ± 9.54vs 35.94 ± 5.27), *p*< 0.001. They also reported that a high correlation was found between the LVEF and GRS. However, they don't determine optimal cutoff.

A well-designed systemic review done by Mangion K *et al*. [21] revealed reduction in global peak radial strain in patients after myocardial infarction which is in line with our study. However, they didn't report cutoff values.

Yu S *et al.* [22] investigated GRS and LVEF in anterior MI patients and showed impaired GCS with preserved function which is agreed with our study. However, they don't determine optimal cutoff value. This the first study to correlate between GRS and LV-EF as well as scar percentage in inferior STEMI patients.

As far as we know this is the first study to correlate between GRS and scar percentage.

To conclude, Our study highlights the CMR-FT derived global radial deformation analyses for LV and its relation to

traditional CMR parameters as well as scar percentage as useful an imaging tools in post MI patients.

Promising advancements in CMR-FT, including multidimensional imaging and AI-driven algorithms, might lead to the creation of a more comprehensive and accurate personalized myocardial performance analysis method.

Conflict of Interest
Not available

Financial Support
Not available

References

1. WHO; c2017: Available from https://www.who.int/news-room/fact-sheets/detail/cardiovascular-diseases.
2. Knuuti J, Wijns W, Saraste A, *et al*. ESC Guidelines for the Diagnosis and Management of Chronic Coronary Syndromes. European Heart Journal. 2020;41(3):407-477.
3. Roes SD, Mollema SA, Lamb HJ, *et al*. Validation of Echocardiographic Two-Dimensional Speckle Tracking Longitudinal Strain Imaging for Viability Assessment in Patients with Chronic Ischemic Left Ventricular Dysfunction and Comparison with Contrast-Enhanced Magnetic Resonance Imaging. American Journal of Cardiology. 2009;104(3):312-317.
4. Wu KC. Myocardial Viability Imaging: Dead or Alive? Journal of the American College of Cardiology. 2012;59(9):836-837.
5. Kim RJ, Wu E, Rafael A, *et al*. The Use of Contrast-Enhanced Magnetic Resonance Imaging to Identify Reversible Myocardial Dysfunction. New England Journal of Medicine. 2000;343(20):1445-1453.
6. Elvanayagam JB, Attila K, Francis JM, *et al*. Value of Delayed-Enhancement Cardiovascular Magnetic Resonance Imaging in Predicting Myocardial Viability After Surgical Revascularization. Circulation. 2004;110(12):1535-1541.
7. Ernst W, Adriana O, Christoph K, *et al*. Magnetic Resonance Low-Dose Dobutamine Test is Superior to Scar Quantification for the Prediction of Functional Recovery. Circulation. 2004;109(18):2172-2174.
8. Schuster A, Hor KN, Kowallick JT, *et al*. Cardiovascular Magnetic Resonance Myocardial Feature Tracking: Concepts and Clinical Applications. Circulation: Cardiovascular Imaging. 2016;9(4):1-9.
9. Biglands JD, Radjenovic A, Ridgway JP. Cardiovascular Magnetic Resonance Physics for Clinicians: Part II. Journal of Cardiovascular Magnetic Resonance. 2012;14(1):66.
10. Davenport MS, Perazella MA, Yee J, *et al*. Use of Intravenous Iodinated Contrast Media in Patients with Kidney Disease: Consensus Statements from the American College of Radiology and the National Kidney Foundation. Radiology. 2020;22(1):85-93.
11. Dillman JR, Ellis JH, Cohan RH, *et al*. Frequency and Severity of Acute Allergic-Like Reactions to Gadolinium-Containing IV Contrast Media in Children and Adults. American Journal of Roentgenology. 2007;189(6):1533-1538.
12. Baessler B, Mannil M, Oebel S, *et al*. Subacute and Chronic Left Ventricular Myocardial Scar: Accuracy of Texture Analysis on Non-Enhanced Cine MR Images. Radiology. 2018;286(1):103-112.
13. Schuster A, Paul M, Bettencourt N, *et al*. Cardiovascular Magnetic Resonance Myocardial Feature Tracking for Quantitative Viability Assessment in Ischemic Cardiomyopathy. International Journal of Cardiology. 2013;162(2):413-420.
14. Claus P, Omar AMS, Pedrizzetti G, *et al*. Tissue Tracking Technology for Assessing Cardiac Mechanics: Principles, Normal Values, and Clinical Applications. Journal of the American College of Cardiology: Cardiovascular Imaging. 2015;8(12):1444-1460.
15. Richardson WJ, Clarke SA, Alexander Quinn T, *et al*. Physiological Implications of Myocardial Scar Structure. Comprehensive Physiology. 2015;5(4):1877-1909.
16. Mangion K, McComb C, Auger DA, *et al*. Magnetic Resonance Imaging of Myocardial Strain After Acute ST-Segment-Elevation Myocardial Infarction: A Systematic Review. Circulation: Cardiovascular Imaging, 2017, 10.
17. Zhang K, Sheu R, Zimmerman NM, *et al*. A Comparison of Global Longitudinal, Circumferential, and Radial Strain to Predict Outcomes after Cardiac Surgery. Journal of Cardiothoracic and Vascular Anesthesia. 2019;33(5):1315-1322.
18. Brady B, King G, Murphy RT, *et al*. Myocardial Strain: A Clinical Review. Irish Journal of Medical Science; c2022.
19. Scatteia A, Baritussio A, Bucciarelli-Ducci C. Strain Imaging Using Cardiac Magnetic Resonance. Heart Failure Reviews. 2017;22:465-476.
20. Tantawy SW, Mohammad SA, Osman AM, *et al*. Strain Analysis Using Feature Tracking Cardiac Magnetic Resonance (FT-CMR) in the Assessment of Myocardial Viability in Chronic Ischemic Patients. International Journal of Cardiovascular Imaging. 2021;37(2):587-596.
21. Yu S, Zhou J, Yang K, *et al*. Correlation of Myocardial Strain and Late Gadolinium Enhancement by Cardiac Magnetic Resonance After a First Anterior ST-Segment Elevation Myocardial Infarction. Frontiers in Cardiovascular Medicine. 2021;8:705487.

How to Cite This Article
Oraby A, Maboud NA, Al-Arabawy R, Dawoud R, Romeih S. Assessment of global radial strain by feature tracking cardiac magnetic resonance in patients with myocardial infarction. International Journal of Radiology and Diagnostic Imaging 2024; 7(2): 62-71.